arXiv:cond-mat/0202411v1 [cond-mat.dis-nn] 22 Feb 2002

Dynamical phase transition in a neural network model with noise: an exact solution

Cristián Huepe and Maximino Aldana-González*

James Franck Institute, University of Chicago, 5640 South Ellis Avenue. Chicago, IL 60637, USA

Submitted to the Journal of Statistical Physics. January, 2002.

Abstract

The dynamical organization in the presence of noise of a Boolean neural network with random connections is analyzed. For low levels of noise, the system reaches a stationary state in which the majority of its elements acquire the same value. It is shown that, under very general conditions, there exists a critical value η_c of the noise, below which the network remains organized and above which it behaves randomly. The existence and nature of the phase transition are computed analytically, showing that the critical exponent is 1/2. The dependence of η_c on the parameters of the network is obtained. These results are then compared with two numerical realizations of the network.

Key words: Neural Network, Phase Transition, Noise, Organization.
Running title: Dynamical phase transition in a neural network with noise.

*Corresponding author. e-mail: maximino@control.uchicago.edu; tel: (773)-702-0946; fax: (773)-702-5863

1 Introduction

Boolean networks have been used to describe a wide variety of complex systems. They provide a common language for models of associative memory [18, 19, 10], spin glasses [17, 4, 15, 5], dynamics of evolution [21, 12, 11], and cellular automata [3, 8, 13, 22]. A typical Boolean network model consists of a set of binary elements (also called nodes, neurons or spins, depending on the context) which are connected among them to form a net. The value of each element at a given time depends on the value at the previous time step of all the nodes that are connected to it.

The use of common tools of statistical physics has revealed a strong parallel between Boolean networks and dynamical systems. In this context, several authors have studied the non-equilibrium dynamics of deterministic Boolean networks and, in particular, the one of *neural networks* [2, 14]. Their work has unveiled the existence of a variety of possible collective behaviors such as synchronized oscillations or chaos [1, 20, 10]. On a similar perspective, the influence of noise on the dynamics of Boolean networks has been analyzed in [16, 9]. It is shown that, for increasing noise level, the barriers separating different attractors decrease and then disappear.

We are interested in considering the changes in the dynamical properties of a deterministic system in the presence of noise. Following this motivation, we study a simple Boolean network model exhibiting self-organization and analyze its tolerance to the effect of noise. We show analytically that the system undergoes a dynamical second-order phase transition as its amount of randomness is increased.

The paper is organized as follows. In section 2, we describe the neural network model with noise. Section 3 introduces the definition of the order parameter characterizing the network and presents numerical evidence for the phase transition by considering two particular network examples. In section 4 we find the dynamical equation satisfied by the order parameter and compute analytically its fixed points, exhibiting the phase transition. In section 5 we apply these results to the two cases studied in section 3. Finally, section 6 is our conclusion.

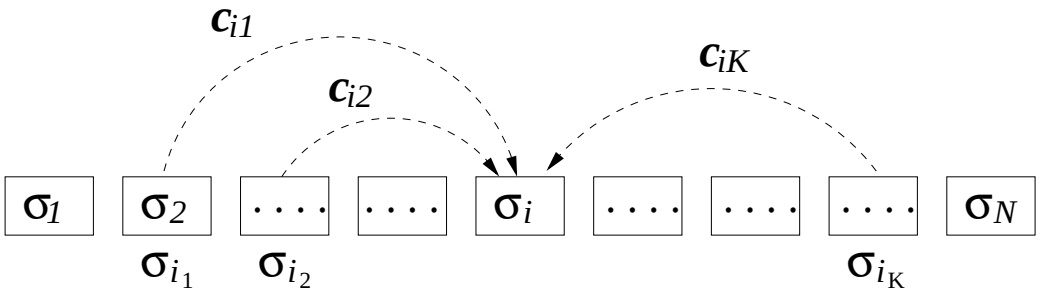


Figure 1: Schematic representation of the structure of the network. Every element σ_i is connected to K other elements $\{\sigma_{i_1}, \ldots, \sigma_{i_K}\}$ (the *linkages*), which are chosen at random from the entire set $\{\sigma_i\}_{i=1\ldots N}$. The contribution of each σ_{i_j} element to the input function of σ_i is weighted by c_{ij} as given in equation (1).

2 Definition of the model

Consider a neural network composed of N elements $\{\sigma_1, \sigma_2, \ldots, \sigma_N\}$, each of which can only take the values $\sigma_i = -1$ or $\sigma_i = +1$. Every σ_i is randomly connected to any K elements of the network, which define its set of *linkages* $\{\sigma_{i_j}\}_{j=1,\ldots,K}$ (see Fig.1). The parameter K is the *connectivity* of the network. Each linkage σ_{i_j} is weighted by an independent random variable c_{ij} that is chosen with a probability density function (PDF) given by $\mathrm{P}_c(x)$. The NK connections of a network, and its corresponding weights, remain fixed throughout the evolution of the system.

At every discrete time step, each σ_i receives a signal $+1$ or -1 equal to the *input function*

$$f\left(c_{i1}, \ldots, c_{iK}; \sigma_{i_1}, \ldots, \sigma_{i_K}\right) = \mathrm{Sign}\left\{\sum_{j=1}^{K} c_{ij}\sigma_{i_j}\right\}. \qquad (1)$$

For the particular case in which we have for all weights $c_{ij} = 1$, this definition corresponds to the *majority rule*, in which f takes the same value as the majority of the linkages.

Using the input function (1), we define a stochastic evolution rule for

every σ_i by introducing a noise intensity η such that

$$\sigma_i(t+1) = \begin{cases} f\left(c_{i1}\dots c_{iK}; \sigma_{i_1}(t)\dots\sigma_{i_K}(t)\right) & \text{with probability } 1-\eta \\ -f\left(c_{i1}\dots c_{iK}; \sigma_{i_1}(t)\dots\sigma_{i_K}(t)\right) & \text{with probability } \eta. \end{cases} \tag{2}$$

The dynamics can thus be set from purely deterministic to purely random by varying η between 0 and 1/2. Note that in the case with $\eta = 0$, the system will typically converge to an ordered state in which all the σ_i are equal.

Due to the presence of noise and to the randomness in the initial assignment of the linkages, the statistical properties of the dynamics of the network do not change if the connection weights or the linkages are either time-independent or if they are randomly re-assigned at every time step. Using the language of boolean networks, this means that for the model presented here the *annealed* and *quenched* dynamics are equivalent [6].

3 Numerical evidence

In this section we perform a numerical study of the evolution of the neural network model introduced above. We show that the system undergoes a dynamical phase transition (for $N \to \infty$) from an ordered to a disordered state as the noise intensity η is increased. The analytical expression for this transition will be deduced in section 4.

Let us define an order parameter that adequately describes the degree of alignment of the elements of the network. We first introduce

$$s(t) = \lim_{N\to\infty}\left[\frac{1}{N}\sum_{i=1}^{N}\sigma_i(t)\right]. \tag{3}$$

With this definition, $|s(t)| \approx 1$ for an "ordered" system in which most elements take the same value, while $|s(t)| \approx 0$ for a "disordered" system in which the elements randomly take values $+1$ or -1. For systems where the time-average of $|s(t)|$ converges, a time-independent order parameter can now be defined as

$$\Psi = \lim_{T\to\infty}\frac{1}{T-T_0}\int_{T_0}^{T}|s(t)|dt, \tag{4}$$

where T_0 can take any arbitrary finite value without changing Ψ.

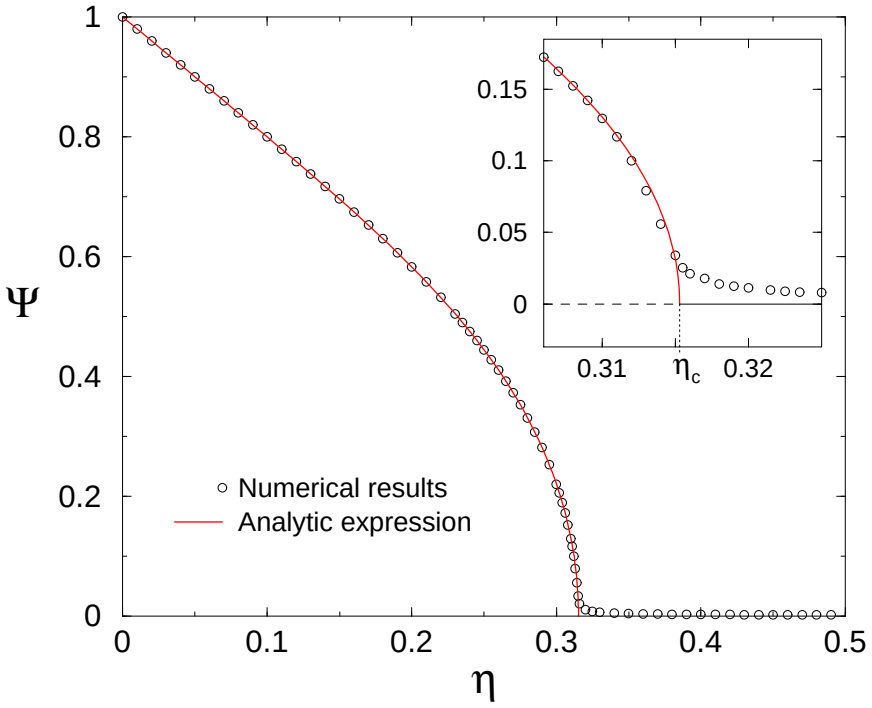


Figure 2: Bifurcation diagram of the order parameter Ψ as a function of the noise intensity η for a neural network model in which $c_{ij} = 1$ for all weights. A phase transition occurs at $\eta_c \simeq 0.3153$. The numeric and analytic results only differ at $\eta \sim \eta_c$, where the blowup shows a slight difference due to finite size effects.

We computed numerically the evolution of the model for a network with $N = 100000$ elements, connectivity $K = 11$, and random initial conditions. In practice, the order parameter Ψ was obtained by integrating $|s(t)|$ from $T_0 = 1000$ (to drop the initial relaxation dynamics) until $T = 10000$. A change to a larger integration time produces negligible variations on the result.

The numerical results presented on Figure 2 show the bifurcation diagram of Ψ as a function of the control parameter η for the case with $c_{ij} = 1$, in which all connection weights are equal. The input function (1) then simply becomes the majority rule. It is apparent that the system undergoes a phase transition at $\eta_c \approx 0.32$. For $\eta < \eta_c$, all elements in the system will tend to align either to $+1$ or to -1. For $\eta > \eta_c$, their values are randomly

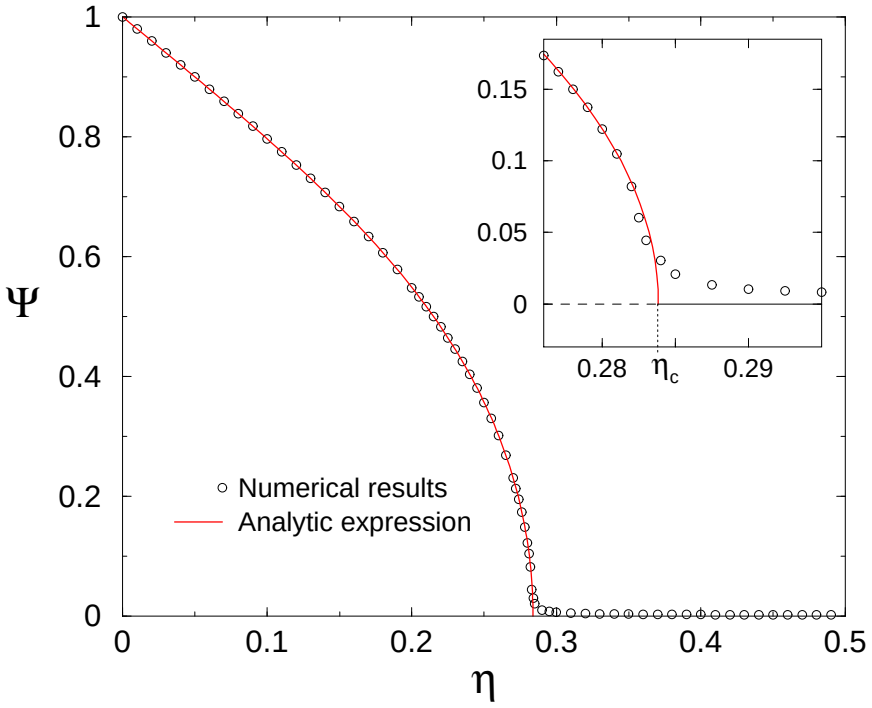


Figure 3: Bifurcation diagram of the order parameter Ψ as a function of the noise intensity η for a neural network model where the weights c_{ij} follow the PDF defined in (5). A phase transition occurs at $\eta_c \simeq 0.2838$. The blowup shows again the differences between the numeric and analytic results due to finite size effects (see Fig. 2).

distributed. The blowup on figure 2 shows the usual finite size effect on the phase transition, which smoothes the curve near η_c.

On figure 3 we present the results for the case of a network with fixed connection weights c_{ij} that follow the PDF

$$\mathrm{P}_c(x) = \begin{cases} 1 & \text{if } 0 \leq x \leq 1 \\ 0 & \text{otherwise.} \end{cases} \tag{5}$$

The phase transition on this system is qualitatively equivalent to the previous one, but the critical noise value is now changed to $\eta_c \approx 0.28$. The blowup shows again the finite size effects.

4 Analytic solution

We will compute here the exact analytic expression that relates the noise intensity control parameter η and the order parameter Ψ for any given PDF of the connection weights $\mathrm{P}_c(x)$.

4.1 Dynamics of the order parameter

First, we will relate the probability distribution of the system at a time $t+1$ with the one at a time t. In order to do so, let us define $\phi_N(t)$ as the fraction of elements in the network whose value is $+1$ at time t:

$$\phi_N(t) = \frac{1}{N}\sum_{i=1}^{N}\frac{\sigma_i(t)+1}{2}. \tag{6}$$

In the thermodynamic limit $N \to \infty$, the above quantity transforms into the probability that at time t any arbitrary node σ_i acquires the value $+1$:

$$\phi(t) \equiv \mathbf{P}_t\{\sigma_i = +1\} = \lim_{N\to\infty}\phi_N(t) \tag{7}$$

Note that from definition (3), the relation between $s(t)$ and $\phi(t)$ is simply given by

$$s(t) = 2\phi(t) - 1. \tag{8}$$

Thus, in a fully ordered state we have $|s(t)| = 1$ and $\phi(t) = 0$ or 1, while in a fully disordered state we have $|s(t)| = 0$ and $\phi(t) = 1/2$.

It is useful to define $\xi_i(t)$ as the argument of the Sign function appearing in the definition of f for the i-th element at a time t (see equation (1)),

$$\xi_i(t) = \sum_{j=1}^{K} c_{ij}\sigma_{i_j}(t). \tag{9}$$

If the linkages of every node are assigned in a sufficiently random way[1], the products $c_{ij}\sigma_{i_j}(t)$ can be considered as independent random variables. Therefore, if we denote by $\mathrm{P}_{\xi(t)}(x)$ and $\mathrm{P}_{c\sigma(t)}(x)$ the PDF associated to ξ_i

[1]If the linkages are not assigned randomly, the situation changes. For example if they are chosen among the first neighbors of every element, there is no phase transition and the analysis presented here is not applicable.

and to the product $c_{ij}\sigma_{i_j}$ respectively, then $\mathrm{P}_{\xi(t)}(x)$ is simply given by the K-fold convolution of $\mathrm{P}_{c\sigma(t)}(x)$ with itself:

$$\mathrm{P}_{\xi(t)}(x) = \underbrace{\mathrm{P}_{c\sigma(t)} * \mathrm{P}_{c\sigma(t)} * \cdots * \mathrm{P}_{c\sigma(t)}(x)}_{K \text{ times}}. \tag{10}$$

In terms of $\mathrm{P}_{\xi(t)}(x)$, the probability $I(t)$ of having the input function $f = +1$ at time t can be computed as

$$I(t) \equiv \mathbf{P}_t \{f = +1\} = \int_0^\infty \mathrm{P}_{\xi(t)}(x)dx. \tag{11}$$

Using the updating rule (2), we can now directly write the probability $\phi(t+1)$ of having $\sigma_i(t+1) = +1$ in terms of $I(t)$ and η:

$$\phi(t+1) = I(t)\,[1-\eta] + [1-I(t)]\,\eta. \tag{12}$$

This master equation describes the stochastic dynamics of the network. Its fixed points as a function of η will generate the bifurcation diagram showing the phase transition.

4.2 Probability distribution of the input function

In order to express equation (12) in a closed form, we must find how $I(t)$ relates to $\phi(t)$. For this, we first compute $\mathrm{P}_{\xi(t)}(x)$ which is in turn determined by $\mathrm{P}_{c\sigma(t)}(x)$. In Fourier space, the convolution appearing in (10) acquires the simple form

$$\hat{\mathrm{P}}_{\xi(t)}(\lambda) = \left[\hat{\mathrm{P}}_{c\sigma(t)}(x)\right]^K, \tag{13}$$

where $\hat{\mathrm{P}}_{\xi(t)}(\lambda)$ and $\hat{\mathrm{P}}_{c\sigma(t)}(\lambda)$ are the Fourier transforms of $\mathrm{P}_{\xi(t)}(x)$ and $\mathrm{P}_{c\sigma(t)}(x)$ respectively.

Since the connection weights c_{ij} are distributed according to the probability function $\mathrm{P}_c(x)$, and the variables $\sigma_i(t)$ evaluate to $+1$ with probability $\phi(t)$ and to -1 with probability $1-\phi(t)$, it follows that the PDF of the products $c_{ij}\sigma_{i_j}$ is given by

$$\mathrm{P}_{c\sigma(t)}(x) = \phi(t)\mathrm{P}_c(x) + [1-\phi(t)]\,\mathrm{P}_c(-x). \tag{14}$$

Taking the Fourier transform of the previous expression, and inserting the result into equation (13), one gets

$$\hat{\mathrm{P}}_{\xi(t)}(\lambda) = \left[\hat{\mathrm{P}}_c^*(\lambda) + \left(\hat{\mathrm{P}}_c(\lambda) - \hat{\mathrm{P}}_c^*(\lambda)\right)\phi(t)\right]^K, \tag{15}$$

where the '*' denotes complex conjugation. From the above expression it is apparent that $\mathrm{P}_{\xi(t)}(x)$, and consequently $I(t)$, are polynomial functions of $\phi(t)$. Therefore, equation (12) is a polynomial of degree K in $\phi(t)$, with solutions that depend on the value of the noise intensity η. As we will see later, the roots of this polynomial will furnish the bifurcation diagram of the order parameter.

For convenience, we will write our results in terms of $s(t)$ instead of $\phi(t)$ (see equation (8)). Substituting $\phi(t) = [s(t)+1]/2$ in expression (15) we get

$$\hat{\mathrm{P}}_{\xi(t)}(\lambda) = \left[\frac{\hat{\mathrm{P}}_c(\lambda) + \hat{\mathrm{P}}_c^*(\lambda)}{2} + \frac{\hat{\mathrm{P}}_c(\lambda) - \hat{\mathrm{P}}_c^*(\lambda)}{2}s(t)\right]^K. \tag{16}$$

By denoting $\hat{g}(\lambda)$ and $\hat{h}(\lambda)$, the real and imaginary parts of $\hat{\mathrm{P}}_c(\lambda)$ respectively, $\hat{\mathrm{P}}_{\xi(t)}(\lambda)$ can then be written as

$$\begin{aligned}\hat{\mathrm{P}}_{\xi(t)}(\lambda) &= \left[\hat{g}(\lambda) + i\hat{h}(\lambda)s(t)\right]^K \\ &= \sum_{m=0}^{K}\binom{K}{m}\left[\hat{g}(\lambda)\right]^{K-m}\left[i\hat{h}(\lambda)s(t)\right]^m,\end{aligned}$$

whose inverse Fourier transform is

$$\mathrm{P}_{\xi(t)}(x) = \sum_{m=0}^{K}\left\{\frac{i^m}{2\pi}\binom{K}{m}\int_{-\infty}^{\infty}\left[\hat{g}(\lambda)\right]^{K-m}\left[\hat{h}(\lambda)\right]^m e^{-i\lambda x}dx\right\}\left[s(t)\right]^m. \tag{17}$$

We are now in position of computing $I(t)$. Using equations (11) and (17), and moving the integrals inside the sum we have

$$I(t) = \sum_{m=0}^{K} a_m\left[s(t)\right]^m, \tag{18}$$

where the a_m are constant coefficients that depend only on $\mathrm{P_c}(\lambda)$ and are given by

$$a_m = \frac{i^m}{2\pi}\binom{K}{m}\int_0^{\infty}\int_{-\infty}^{\infty}\left[\hat{g}(\lambda)\right]^{K-m}\left[\hat{h}(\lambda)\right]^m e^{-i\lambda x}\,d\lambda\,dx. \tag{19}$$

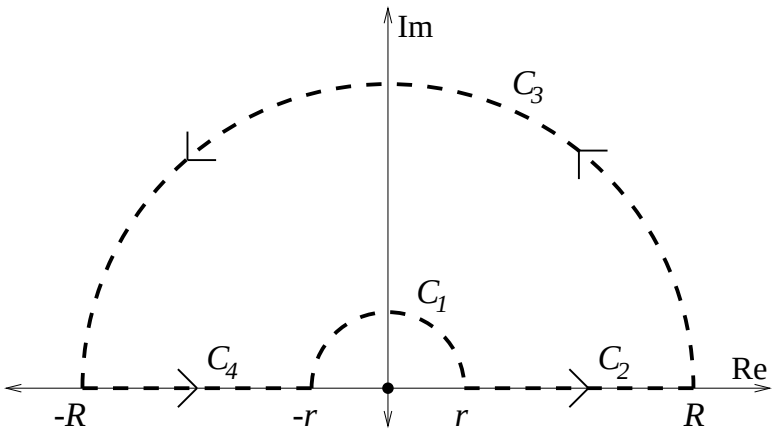


Figure 4: Integration contour $\mathcal{C}$ on the complex plane that was used to compute (21). The pole at the origin is circumvented by the half-circle $\mathcal{C}_1$ of radius r.

We can formally integrate over x by replacing $e^{-i\lambda x} \to e^{-(i\lambda+\epsilon)x}$, computing the new x-integral, and then evaluating the result at $\epsilon = 0$. Our final formula for the a_m coefficients gives

$$a_m = \frac{-i^{m+1}}{2\pi}\binom{K}{m}\int_{-\infty}^{\infty}\frac{1}{\lambda}\left[\hat{g}(\lambda)\right]^{K-m}\left[\hat{h}(\lambda)\right]^{m}d\lambda. \tag{20}$$

Note that $a_m = 0$ for all even values of m. Indeed, since the function $\hat{g}(\lambda)$ is even and $\hat{h}(\lambda)$ is odd, the integrand will be antisymmetric for any even m, thus vanishing the integral.

It will be useful for later calculations to compute the value of a_0. In fact, it turns out that $a_0 = 1/2$ for every K and any "well behaved" function $\mathrm{P_c(x)}$. This can be readily proven by extending the integral in (20) to the complex plane. The integration path $\mathcal{C}$ shown on figure 4 contains no poles, therefore

$$\oint_{\mathcal{C}}\frac{1}{z}\left[\hat{g}(z)\right]^{K}dz = 0. \tag{21}$$

Since $\mathrm{P}_c(x)$ is a PDF, Parseval's theorem guarantees that its Fourier transform is square integrable, which implies $\int_{-\infty}^{\infty}\hat{g}^2(\lambda)d\lambda < \infty$. Therefore, the contribution of segment $\mathcal{C}_3$ to the integral in (21) is zero for $R \to \infty$. On the other hand, being $\hat{g}(\lambda)$ the real part of the Fourier transform of a PDF, one has $\hat{g}(0) = 1$ and thus, for any well behaved function it is possible to

approximate $\hat{g}(r) \simeq 1$ over the small segment $\mathcal{C}_1$. This allows us to compute $\int_{\mathcal{C}_1} \frac{1}{z} [\hat{g}(z)]^K \, dz = \int_{\pi}^{0} i d\theta = -i\pi$. Replacing into (21), we obtain the value of the integral in (20) and find that $a_0 = 1/2$ for any $\mathrm{P}_c(x)$ and any K.

4.3 Computing the bifurcation diagram

We can now combine the main results of sections 4.1 and 4.2 to find an analytic expression relating η and Ψ. We have shown that $I(t)$ is a polynomial of degree K in $s(t)$. Therefore, in terms of $s(t)$, the master equation (12) governing the dynamics of the network becomes

$$s(t+1) = 2\,(1-2\eta)\left(a_1 s(t) + a_3[s(t)]^3 + \cdots + a_K[s(t)]^K\right). \qquad (22)$$

In the limit $t \to \infty$, $s(t)$ will asymptotically approach a fixed point s which, from the above equation, obeys

$$s = 2\,(1-2\eta)\left(a_1 s + a_3 s^3 + \cdots + a_K s^K\right). \qquad (23)$$

It is important to point out that if the probability function $\mathrm{P_c(x)}$ is symmetric, there is no phase transition. Indeed, if $\mathrm{P_c(x)}$ satisfies $\mathrm{P_c(x) = P_c(-x)}$, then the imaginary part $\hat{h}(\lambda)$ of its Fourier transform would be identically zero. It follows from equation (20) that $a_m = 0 \; \forall \; m$ and, therefore, equations (22) and (23) give the trivial result $s = 0$ as the only possible solution for the dynamics.

Equation (23) is always satisfied by $s = 0$. However, as η is varied, this solution becomes unstable as other ones appear. Discarding the solution $s = 0$ and solving equation (23) for η, we get

$$\eta = \frac{a_1 - 1/2 + a_3 s^2 + \cdots + a_K s^{K-1}}{2(a_1 + a_3 s^2 + \cdots + a_K s^{K-1})}. \qquad (24)$$

By dividing the polynomials and neglecting the terms of order s^4 and higher in the resulting expression[2], we obtain

$$\eta - \eta_c = \frac{a_3}{4a_1^2} s^2 \qquad (25)$$

[2]As it can be seen in figures 2 and 3, the order parameter vanishes continuously when passing from the ordered to the disordered phase. Therefore, in the vicinity of the phase transition $s \approx 0$.

where η_c is defined as

$$\eta_c = \frac{1}{2}\left(1 - \frac{1}{2a_1}\right). \tag{26}$$

Since $a_3 < 0$, equation (25) implies that real non-zero solutions for s in (23) only exist if $\eta < \eta_c$. For $\eta > \eta_c$ the solutions of equation (25) are imaginary and therefore $s = 0$ is the only acceptable solution of (23). We thus conclude that a phase transition with critical exponent 1/2 will occur at $\eta = \eta_c$. The explicit behavior of the order parameter $\Psi = |s|$ near the transition will be

$$\Psi = \begin{cases} \frac{2a_1}{\sqrt{|a_3|}}\left(\eta_c - \eta\right)^{1/2} & \text{for} \quad \eta < \eta_c \\ \\ 0 & \text{for} \quad \eta > \eta_c \end{cases} \tag{27}$$

5 Examples of the analytic solution

In this section we compare our analytic solution with the numerical results presented in section 3.

We consider first the case with $c_{ij} = 1$ for all connections. The PDF of these connection weights is then $\mathrm{P_c}(x) = \delta(x-1)$, and we have

$$\hat{\mathrm{P}}_c(\lambda) = \int_{-\infty}^{\infty} \delta(x-1) e^{i\lambda x} dx = \cos(\lambda) + i\sin(\lambda). \tag{28}$$

Therefore, the coefficients a_m are given by

$$a_m = \frac{-i^{m+1}}{2\pi}\binom{K}{m}\int_{-\infty}^{\infty} \frac{1}{\lambda}\left[\cos(\lambda)\right]^{K-m}\left[\sin(\lambda)\right]^m d\lambda. \tag{29}$$

For the other case, in which the connection weights are uniformly distributed in the interval $[0, 1]$ as given in expression (5), we get

$$\hat{\mathrm{P}}_c(\lambda) = \int_0^1 e^{i\lambda x} dx = \frac{\sin(\lambda)}{\lambda} + i\frac{1-\cos(\lambda)}{\lambda}, \tag{30}$$

and the corresponding coefficients a_m are given by

$$a_m = \frac{-i^{m+1}}{2\pi}\binom{K}{m}\int_{-\infty}^{\infty} \frac{1}{\lambda^{K+1}}\left[\sin(\lambda)\right]^{K-m}\left[1-\cos(\lambda)\right]^m d\lambda. \tag{31}$$

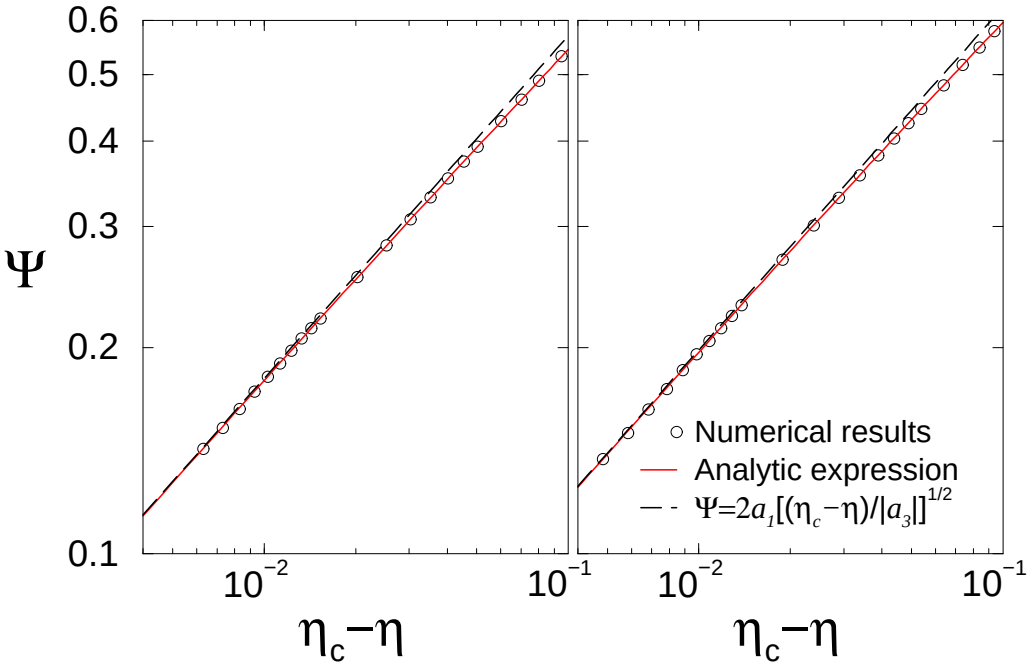


Figure 5: Log-log plot of the order parameter Ψ as a function of the distance to the critical noise value $\eta_c - \eta$. The left side graph corresponds to the case with equal connection weights $c_{ij} = 1$. The right hand graph is for uniformly distributed connection weights. The values of $\eta_c = 0.3153$ (left) and $\eta_c = 0.2838$ (right) were obtained from equation (26). The numerical results (circles) and the analytic solution (solid line) approach asymptotically the dashed line representing the bifurcation form (27).

We evaluated the integrals in (29) and (31) for the case $K = 11$, which was studied in section 3. By replacing them into equation (24) we explicitly obtain η as a function of s for these two particular cases. The solid curves on figures 2 and 3 show the analytic bifurcation diagram that is found through this procedure. The agreement with the results our numerical simulation is excellent, confirming our assumption that all elements can be considered as independent random variables, even if the network connections and weights are kept fixed throughout the evolution of the system.

Once the values of the coefficients a_m are obtained, the critical noise value η_c can be readily calculated by using equation (26). Figure 5 shows a log-log

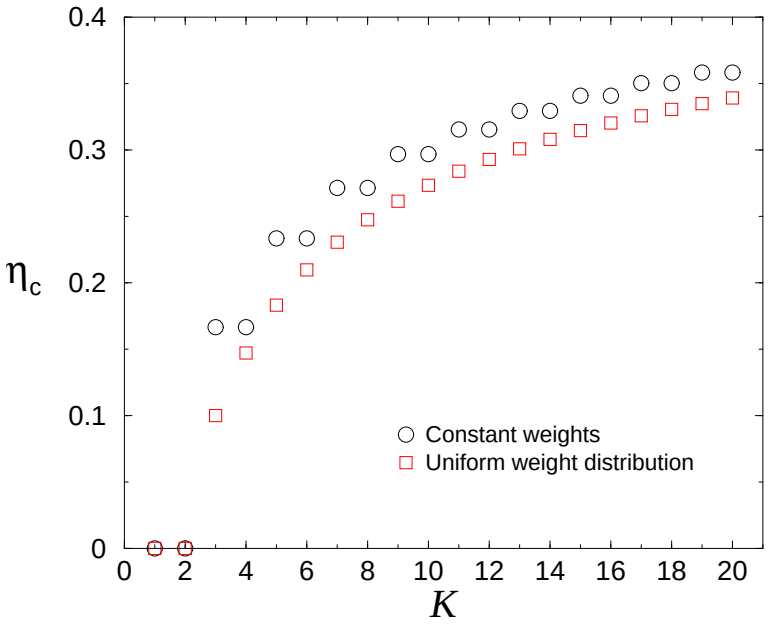


Figure 6: Critical noise level η_c for various values of the connectivity K and two different weight distributions: $c_{ij} = 1$ for all connections (circles) and c_{ij} uniformly distributed in $[0, 1]$ (squares). As the connectivity increases, the amount of noise needed to disorganize the system must increase. For large K, the value of η_c will tend asymptotically to the maximum noise level $1/2$. For $K \leq 2$ both cases have $\eta_c = 0$, and the system becomes disorganized for any noise $\eta > 0$. In the constant weight case, the values of η_c at consecutive odd and even values of K are equal (see text).

graph of the vanishing value of Ψ as a function of $\eta_c - \eta$, both for the constant connection weight case ($\eta_c \simeq 0.3153$) and for the uniform distribution weight case ($\eta_c \simeq 0.2838$). These results are the same that were presented in section 3. On the displayed windows, finite-size effects around η_c are not visible. As can be seen on this figure, the numerical results coincide perfectly with the analytic solution (24) (solid curve) and with the asymptotic behavior given in (27) (dashed line).

Figure 6 shows the critical noise level η_c as a function of the connectivity K for the two particular cases studied. As the connectivity is increased, the phase transition appears at higher levels of noise and it is increasingly hard

to disorder the system. As the system becomes more and more correlated, η_c will asymptotically approach its maximum value of 1/2 (data not shown). For the case in which $c_{ij} = 1$ for all connections, the majority rule is not well defined for even values of K, since there can be equal number of elements with $\sigma_i = +1$ and $\sigma_i = -1$. This justifies the degeneracy observed for η_c with respect to consecutive odd and even values of K. For $K = 2$ the system will be disorganized at any $\eta_c > 0$ and no phase transition occurs.

6 Conclusions

We have shown the existence of a noise-driven phase transition in a neural network with random connections. We found an exact analytic solution of the stochastic equation which governs the dynamics of the system. By finding its fixed points as a function of noise we constructed the bifurcation diagram, which shows that the phase transition is of second-order with a critical exponent of 1/2.

Besides the randomness of the network connection, our work was carried out with very few assumptions. One of these was to consider the connection weights as statistically independent variables. This condition, however, is not satisfied by many models of interest such as the Hopfield neural networks [10]. It would therefore be of great interest to generalize our approach to cases in which the connection weights are statistically correlated. Given that these conditions are satisfied, the existence of the phase transition only seems to require that the PDF of the connection weights $\mathrm{P}_c(x)$ is a non-symmetric but otherwise arbitrary function, as shown on section 4.3.

The general framework under which the results on this paper were derived leads us to believe that this type of noise-driven phase transitions from an ordered to a disordered state must be a robust feature of systems with elements that are somehow randomly connected [7].

Acknowledgements

We would like to thank Leo Kadanoff for his encouragement and valuable scientific discussions. This work was supported in part by the MRSEC Program of the National Science Foundation under award number 9808595, and

by the NSF DMR 0094569. M. Aldana also acknowledges CONACyT-México for a postdoctoral grant and the Santa Fe Institute of Complex Systems for partial support through the David and Lucile Packard Foundation Program in the Study of Robustness.

References

[1] H. D. I. Abarbanel, M. I. Rabinovich, A. Selverston, and M. V. Bazhenov. Synchronization in neural networks. *Physics-Uspeki*, 39(4):337–362, 1996.

[2] B. Cheng and D. M. Titterington. Neural networks: a review from a statistical perspective. *Statistical Science*, 9(1):2–54, Feb 1994.

[3] J. A. De Sales, M. L. Martins, and D. A. Stariolo. Cellular automata model for gene networks. *Physical Review E*, 55(3):3262–3270, Mar 1997.

[4] B. Derrida. Dynamical phase transitions in non-symmetric spin glasses. *Journal of Physics A: Mathematical and General*, 20:L721–L725, 1987.

[5] B. Derrida and H. Flyvbjerg. Multivalley structure in kauffman model - analogy with spin-glasses. *Journal of Physics A: Mathematical and General*, 19(16):1003–1008, Nov 1986.

[6] B. Derrida and Y. Pomeau. Random networks of automata - a simple annealed approximation. *Europhysics Letters*, 1(2):45–49, Jan 1986.

[7] J. Doyne Farmer. A roseta stone for connectionism. *Physica D*, 42(1-3):153–187, Jun 1990.

[8] H. Flyvbjerg. Recent results for random networks of automata. *Acta Physica Polonica B*, 20(4):321–349, Apr 1989.

[9] O. Golinelli and B. Derrida. Barrier heights in the kauffman model. *Journal De Physique*, 50(13):1587–1601, Jul 1989.

[10] J. J. Hopfield. Neural networks and physical systems with emergent collective computational abilities. *Proceedings of the National Academy of Sciences*, 79(8):2554–2558, Apr 1982.

[11] Stuart A. Kauffman. Metabolic stability and epigenesis in randomly constructed nets. *Journal of Theoretical Biology*, 22:437–467, 1969.

[12] Stuart A. Kauffman. *The Origins of Order: Self-Organization and Selection in Evolution*. Oxford University Press, Oxford, 1993.

[13] K. E. Kürten. Correspondence between neural threshold networks and kauffman boolean cellular automata. *Journal of Physics A: Mathematical and General*, 21(11):L615–L619, Jun 1988.

[14] K. E. Kürten. Critical phenomena in model neural netwoks. *Physics Letters A*, 129(3):157–160, May 1988.

[15] M. Mezard, G. Parisi, and M. A. Virasoro. *Spin Glass Theory and Beyond*. World Scientific, Singapore, 1987.

[16] E. N. Miranda and N. Parga. Noise effects in the kauffman model. *Europhysics Letter*, 10(4):293–298, Oct 1989.

[17] D. Petters. Patch algorithms in spin glasses. *International Journal of Modern Physics C*, 8(3):595–600, Jun 1997.

[18] K. Sakai and Y. Miyashita. Neural organization for the long-term-memory of paired associates. *Nature*, 354(6349):152–155, Nov 1991.

[19] D. Sherrington and K. Y. M. Wong. Random boolean networks for autoassociative memory. *Physics Reports: Review Section of Physics Letters*, 184(2-4):293–299, Dec 1989.

[20] Lipo Wang, Elgar E. Pichler, and John Ross. Oscillations and chaos in neural networks - an exactly solvable model. *Proceedings of the National Academy of Sciences of the United States of America*, 87(23):9467–9471, Dec 1990.

[21] Claus O. Wilke, Cristopher Ronnenwinkel, and Thomas Martinetz. Dynamic fitness landscapes in molecular evolution. *Physics Reports*, 349(5):395–446, Aug 2001.

[22] Stephen Wolfram. Statistical mechanics of cellular automata. *Reviews of Modern Physics*, 55(3):601–644, Jul 1983.